2025 IEEE/SICE International Symposium on System Integration (SII)
January 21-24, 2025, Munich, Germany

Derivation of Optimal Insertion Speed for Organs to Satisfy Efficiency and Accuracy

Hiroyasu Iwata, *Member, IEEE*, Ryusuke Hamano, Kechao Yu, Ryohei Saito

***Abstract*— While administering cancer vaccines, an extra-fine needle punctures into the affected area. Reportedly, needle insertion speeds affect the insertion reaction force, causing needle deflections. Additionally, longer insertion times increase the effect of respiratory fluctuations on the needle insertion speeds, leading to a reduction in needle deflections. This study focused on deriving the optimal speed for the liver, kidney, fat, and muscle of pigs to enable efficient and accurate insertion. Insertion tests were conducted to analyze the dependence of needle deflections on the insertion speed ranging from 2 to 20 mm/s and insertion angles of 0°, 15°, 30°, and 45°. Subsequently, a diagram of the relationship among insertion speeds, insertion angles, and needle deflections was created for each organ; this illustration, suggests that it is possible to determine the optimal insertion speed. In future, it is necessary to derive the optimal insertion speed for organs not used in this study. It is desirable to use insertion planning in combination with organ segmentation techniques using computed tomography (CT) images to optimal insertion speed.**

I. Introduction

Fine needle insertion has been explored for minimally invasive medical applications such as ablation therapy, brachytherapy, drainage, and local anesthesia. Recently, its use has been examined in cancer vaccine therapies using autogenetic dendritic cells, which have been proposed as new cancer treatment methods with few side effects. It is hypothesized that the cancer vaccines are most effective when the autogenetic dendritic cells in a vaccine are injected directly into a tumor [1]. This therapy is applicable to lymphatic malignancies which can easily spread to other parts of the body and must be cured at an early stage. However, accurate needle insertion into a tumor is difficult because a fine needle can be easily deflected. In the past, researchers have tried to assist percutaneous needle insertion using robot systems [2]. Although many studies have focused on the prostate and liver, none of them have examined abdominal insertion in detail [3]–[6].

*Research supported by Hasumi International Research Foundation.

H. Iwata is with the Faculty of Science and Engineering, Waseda University, 27 Waseda-cho, Shinjuku-ku, Tokyo 162-0042, Japan (E-mail: jubi@waseda.jp).

R. Hamano is with Graduate School of Creative Science and Engineering, Waseda University, 27 Waseda-cho, Shinjuku-ku, Tokyo 162-0042, Japan (corresponding author , E-mail: reones@fuji.waseda.jp).

K. Yu is with Graduate School of Creative Science and Engineering, Waseda University, 27 Waseda-cho, Shinjuku-ku, Tokyo 162-0042, Japan (E-mail: yukachou@toki.waseda.jp).

R. Saito is with Graduate School of Creative Science and Engineering, Waseda University, 27 Waseda-cho, Shinjuku-ku, Tokyo 162-0042, Japan (E-mail: ryohei.0729.fly@akane.waseda.jp).

Therefore, our group aimed to develop a needle insertion robot to assist with cancer vaccine administration, particularly focusing on lower abdominal puncture. When an extra-fine needle is inserted into a lymph node at the lower abdomen, it will pass through multiple tissues, such as the skin, fat, muscle, and large and small bowels, which have diverse properties. In particular, membranous organs, such as the intestine, differ significantly from parenchymal organs, such as muscles, in terms of undergoing tissue deformation and forming needle force patterns during needle insertion.

In recent years, considerable research has been conducted on steering the needle tip with axial rotation [7]–[9]. It is necessary to obtain real-time information on the position of the needle tip and tumor to control the needle tip. Several control methods have been proposed based on the information obtained using ultrasound diagnostic equipment. However, the application of diagnostic ultrasound equipment is complicated because intestinal gas causes the attenuation of ultrasound.

Hence, it is essential to apply computed tomography (CT), which can capture clear images of deep parts of the body to help guide the needle insertion. Furthermore, CT uses ionizing radiation. Hence, accurate needle insertion into the tumor under low-frequency CT imaging is crucial for effectively minimizing the number of scans required to determine the position of needle insertion.

In previous studies, the estimation of needle deflections was based on tissue properties, such as needle insertion speeds, insertion reaction forces around the needle tip and needle shaft, and viscoelastic forces [7], [10]–[12]. In multiple insertion simulations, models were developed based on the assumption that the tissue surface, tissue deformation, and insertion force required to break tissue viscoelasticity are constant. However, actual biomaterials have uncertain properties such as heterogeneity and nonlinearity. As the interaction forces between the needle and the tissue vary owing to unexpected tissue, blood vessels, and membrane ruptures, as well as needle tip slipping, the needle often cannot be inserted along the ideal insertion path. Because of all these uncertain factors, it is impractical to develop a method to estimate needle deflections accurately. In particular, when inserting a needle into the abdomen, there are numerous uncertainties because the insertion path includes the intestines.

Therefore, when inserting a needle specific for the lower abdomen into a lymph node, we need to make a pre-operative plan based on CT images, minimize needle insertion deflections, and adopt an approach that inserts an extra-fine needle in a straight direction. Therefore, it is essential to develop a control method that ensures minimal needle deflections and optimizes the insertion position. However,

improper insertion speed, insertion angle, respiratory variability, and the use of extra-fine needles can cause needle deflections and reduce insertion accuracy during insertion. Previous studies have shown that the insertion angle causes nonuniformity in the reaction force from the tissue, resulting in needle deflections and slippage [13]–[16]. Meanwhile, it has been reported that insertion speed causes deflections [17]–[21]. While needle deflections can be minimized by performing high-speed insertion with 18G needles [18], high-speed insertion cannot be used for extra-fine needle insertion due to needle breakage and buckling. While a study suggests that needle deflections increase with rising insertion speeds for soft tissues [20], another study suggested that there is a specific critical insertion speed at which needle deflections are minimized with increasing insertion speed for transrectal prostate brachytherapy [21]. These studies investigated the relationship between insertion speeds and deflections and did not determine an optimal insertion speed. Thus, we believe that different organs require different optimal insertion speeds and have different propensities for increasing the insertion speed. In addition, longer insertion times are considered to lower insertion accuracy because needle deflections are strongly affected by respiratory variability. Therefore, it is necessary to take countermeasures such as considering the insertion speed. However, it is currently set based on empirical rules.

In this study, we evaluated insertion deflections in different organs at various insertion angles with varying insertion speeds, and experimentally clarified the optimal insertion speed for organs with. Previously, we have confirmed that needle deflections can be reduced by adding bi-directional rotation and progressive vibration to the needle [13]. Therefore, we added these techniques to all the needle insertions in this study. Furthermore, an insertion planning system relying on appropriate insertion speeds for each organ was devised to improve insertion accuracy and reduce time. The system's goal is to reduce the burden on the physicians using the system. The main technology of the insertion planning system is the automatic identification of organ types and boundaries on CT images.

II. Effects of Insertion Speed

A. Experimental Setup

Fig. 1 describes the experimental setup used in this study. **Fig. 1** (a) depicts a plate with four square holes used in experiments. **Fig. 1**(b) shows the needle being inserted into an organ whose displacement is restricted by agar fixed to a plate and placed around the organ. The needle is punctured so that it passes through the four holes in the plate, the plate is drilled with four square holes so that the needle does not follow the same insertion path even if the number of insertion attempts is high. **Fig. 1** (c) depicts an experimental system in which insertion deflections were measured by photographing the needle from two orthogonal directions. An example of an image captured by the camera is shown in **Fig. 1** (d). As illustrated in **Fig. 2**, insertions were performed with an organ not on the plate and with the organ on the plate, respectively, and needle deflections were determined by calculating the distance between the needle tip at the ideal point and the real

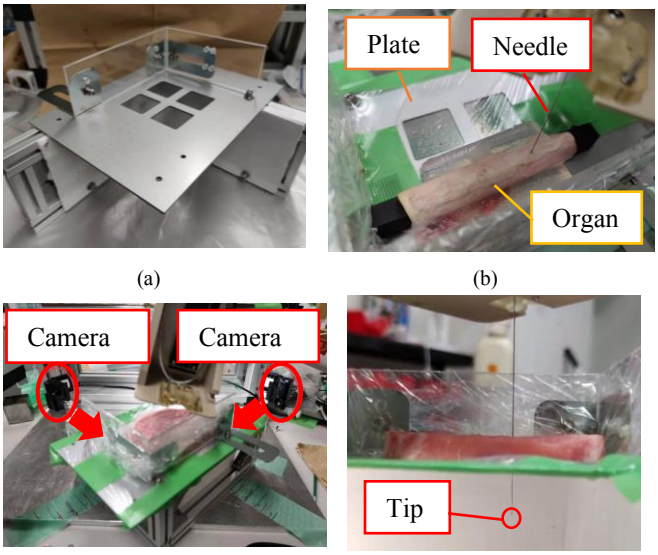

Figure 1. Experimental setup.
(a) A plate with four square holes was used in experiments.
(b) Needle insertion was performed on an organ fixed on a plate with four square holes.
(c) Needle deflection was measured in the experimental system using two cameras.
(d) Examples of images acquired by the cameras.

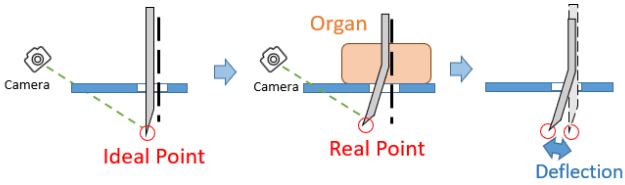

Figure 2. Method of calculating needle deflection.
(a) Measure ideal needle tip position by passing the needle through the hole in the plate without placing the organ.
(b) The organ is fixed on a plate and a needle insertion is performed to measure the needle tip position at which deflection occurs.
(c) Needle deflection is calculated by calculating the distance between the ideal needle tip position and the needle tip position where deflection actually occurred.

point. Two-dimensional deflections could be calculated from the images taken by the cameras, and three-dimensional deflections could be calculated from the two-dimensional deflections calculated by each camera by taking images from two orthogonal directions using the Pythagorean theorem.

We have been developing a robot that puncture the abdomen [13]–[16]. Therefore, in this study, we targeted the liver and kidney, the major organs of the abdomen, as well as fat and muscle, tissues that a needle punctures through during the insertion. Hence, insertion tests with bi-directional rotation and progressive vibration added to 25-gauge needles were performed on the fat, muscle, liver, and kidney of pigs, which have body structures similar to those in humans. For each organ, the insertion angle was 0°, and the insertion distance was 80 mm, which allowed passage through all organs. The insertion distance was the vertical distance in the insertion, and the insertion depth after passing through the organs was fixed at 30 mm. The insertion speed varied from

2 to 20 mm/s in 2-mm/s increments, and 12 insertion tests were performed under each condition. In the case of a tumor with a diameter of 10 mm, the needle's deflection for sufficient insertion is 2.50 mm. Three samples were prepared for each organ, and insertion were made at four different sites in each sample. The experiments were performed at room temperature.

B. Results on Pig Fat

For the relationship between insertion speeds and needle deflections in the insertion tests on a pig fat (data not shown), the Pearson correlation coefficient was 0.236. Thus, there was no significant difference between the two. The mean needle deflection was 1.62 mm. The mean needle deflection reached the maximum at insertion speed of 18 mm/s, its value was 2.00 mm and less than 2.50 mm. Thus, a faster insertion speed can improve the efficiency of puncturing into pig fat without significantly decreasing insertion accuracy.

C. Results on Pig Liver

For the relationship between insertion speeds and needle deflections in the insertion tests on the pig liver (data not shown), the Pearson correlation coefficient was 0.118. Thus, there was no significant difference between the two. The mean value of needle deflection was 1.58 mm. The mean needle deflection reached the maximum at the insertion speed of 12 mm/s, its value was 1.74 mm and less than 2.50 mm. Thus, a faster insertion speed can improve the insertion efficiency of pig liver without significantly decreasing insertion accuracy.

D. Results on Pig Kidney

The relationship between insertion speeds and needle deflections when the needle was inserted into a pig kidney is shown in **Fig. 3**. The trend of the changes in insertion speeds was divided into two ranges: 2–12 mm/s and 14–20 mm/s. The Kolmogorov–Smirnov test was performed for both ranges. In the 2–12 mm/s range, the *p*-value was 0.001, indicating a significant difference in needle deflections. In this range, needle deflections decreased with increasing insertion speeds. In the second range between 14–20 mm/s, the *p*-value was 0.009, also revealing a significant difference in needle deflections. In this range, needle deflections increased with increasing insertion speeds. Therefore, the mean needle deflection at an insertion speed of 12 mm/s was 1.84 mm, which was found to be an optimal insertion speed if prioritizing insertion accuracy.

E. Experiment on Pig Muscle

Fig. 4 depicts the relationship between insertion speeds and needle deflections when the needle is inserted into pig muscle. Similar to the previous section, the trend of change in the needle deflections was divided into two ranges: 2–10 mm/s and 12–20 mm/s. The Kolmogorov–Smirnov test was performed for both ranges. The first range exhibited the *p*-value of 0.001, indicating a significant difference in needle deflections. In this range, needle deflections decreased with increasing insertion speeds. In the second range, the *p*-value was 0.020, indicating a negligible equal variance. Therefore, a

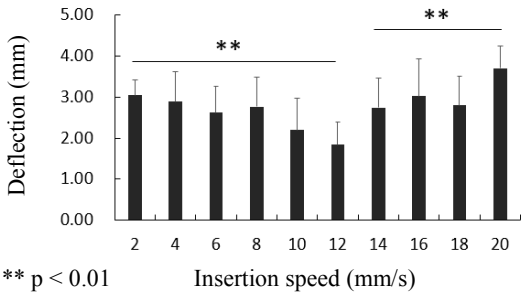

Figure 3. Relationship between insertion speeds and needle deflections in the pig kidney.

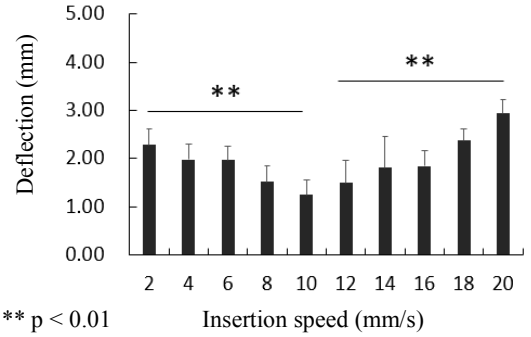

Figure 4. Relationship between insertion speeds and needle deflections in pig muscle.

durability test of mean equivalence (Welch's test) was conducted, which resulted in the *p*-value of 0.007, revealing a significant difference. In this range, needle deflections increased with increasing insertion speeds. Therefore, the mean needle deflection at an insertion speed of 10 mm/s was 1.25 mm, which was found to be an optimal insertion speed if prioritizing insertion accuracy.

F. Discussion

No critical insertion speed was found for needle deflections in pig fat and liver at an insertion angle of 0°. Since pig fat and liver are soft, it was thought that the rupture stress would be low and that even slow insertion speeds could add sufficient force to cut the tissue. Even if the insertion speed was increased, no significant increase in deflections was expected to occur because the reaction force that caused deflections in soft organs was small.

In contrast, a critical insertion speed was found for needle deflection at an insertion angle of 0° in pig kidney and muscle. Because pig fat and liver were hard, the rupture stress was high, so it would take time to cut the tissue at insertion speeds less than the critical insertion speed; the time taken would cause needle deflections. Therefore, increasing the insertion speed was thought to ease the cutting of the tissue and reduce needle deflections. Conversely, if the insertion speed was increased excessively, needle deflection was thought to increase significantly because the reaction force causing deflections in hard organs would increase.

III. Effects of the Insertion Angle

A. Experimental Setup

In this section, we tested whether the optimal insertion speed for an organ would alter with changing insertion angles. The experiments described in this section were conducted using the experimental system described in the previous section. Again, the relationship between insertion angles and needle deflections was investigated using pig fat, muscle, kidney, and liver. In this section, the same insertion tests as in the previous section were performed at six different insertion speeds (2, 4, 6, 8, 10, and 20 mm/s) at four different insertion angles (0°, 15°, 30°, and 45°), and 12 insertion experiments were conducted for each condition.

B. Results on Pig Fat

Fig. 5 illustrates the relationship between needle deflections and the combination of insertion speeds and insertion angles when pig fat was punctured. The mean needle deflections 1.53, 2.65, 3.77, and 6.10 mm for insertion angles at 0°, 15°, 30°, and 45°, respectively. The *p*-value of the Gisser–Greenhouse correction from 0° to 45° was less than 0.001, suggesting a significant difference. Also, the *p*-value of the Bonferroni's multiple comparison test between 0° and 15°, 15° and 30°, and 30° and 45° was less than 0.001, indicating a significant difference. Thus, needle deflections appeared to increase as the insertion angles increased. In addition, the changing behavior of needle deflections with increasing insertion speeds varied for different insertion angles. At an insertion angle of 15°, needle deflections only at 6, 10, and 20 mm/s were less than 2.5 mm. At other insertion speeds, needle deflections were greater than 2.5 mm. At 30° and 45°, needle deflections were greater than 2.5 mm under both conditions.

C. Results on Pig Liver

Fig. 6 depicts the relationship between needle deflections and the combination of insertion speeds and insertion angles when the pig liver was punctured. The mean needle deflections were 1.55, 3.10, 4.39, and 12.19 mm for insertion angles at 0°, 15°, 30°, and 45°, respectively. The *p*-value of the Gisser–Greenhouse correction from 0° to 45° was less than 0.001, indicating a significant difference. In addition, the *p*-value of Bonferroni's multiple comparison test p-value between 0° and 15°, 15° and 30°, and 30° and 45° was less than 0.001, suggesting a significant difference. Thus, needle deflections appeared to increase as the insertion angles increased. Additionally, the changing behavior of needle deflections with increasing insertion speeds was different for insertion angles. At the insertion angle of 15°, needle deflections were less than 2.5 mm only at 2 and 4 mm/s. At other insertion speeds, needle deflections were greater than 2.5 mm. At 30° and 45°, needle deflections were greater than 2.5 mm.

D. Results on Pig Kidney

Fig. 7 describes the relationship between needle deflections and the combination of insertion speeds and insertion angles when the pig kidney was punctured. The mean needle deflections were 2.87, 2.83, 4.38, and 7.32 mm, for insertion angles at 0°, 15°, 30°, and 45°, respectively. The *p*-value for Gisser–Greenhouse correction p-value from 0° to 45° was less than 0.001, suggesting a significant difference. In addition, the p-value of Bonferroni's multiple comparison test *p*-value between 0° and 15° was 1.000, indicating no significant difference. The *p*-value for Bonferroni's multiple comparison test between 15° and 30°, and 30° and 45° was less than 0.001, noting a significant difference. Thus, needle deflections were not significantly affected by small insertion

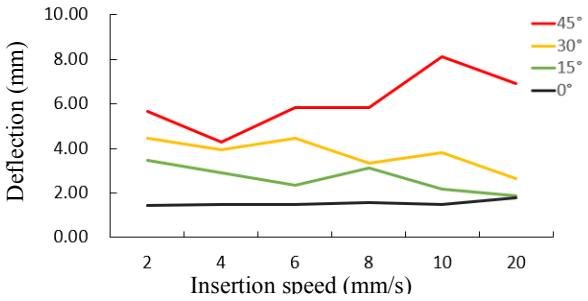

0° to 45° : Greenhouse-Geisser $p < 0.001$ **
0° and 15° : Bonferroni $p < 0.001$ **
15° and 30° : Bonferroni $p < 0.001$ **
30° and 45° : Bonferroni $p < 0.001$ **

Figure 5. Needle deflections due to the combination of insertion angles and insertion speeds in pig fat. The legend in the upper right corner of the figure indicates the four insertion angles (0°, 15°, 30°, and 45°).

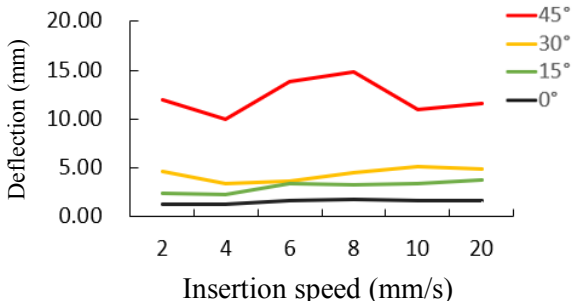

0° to 45° : Greenhouse-Geisser $p < 0.001$ **
0° and 15° : Bonferroni $p < 0.001$ **
15° and 30° : Bonferroni $p < 0.001$ **
30° and 45° : Bonferroni $p < 0.001$ **

Figure 6. Needle deflections due to the combination of insertion angles and insertion speeds in pig liver. The legend in the upper right corner of the figure indicates the four insertion angles (0°, 15°, 30°, and 45°).

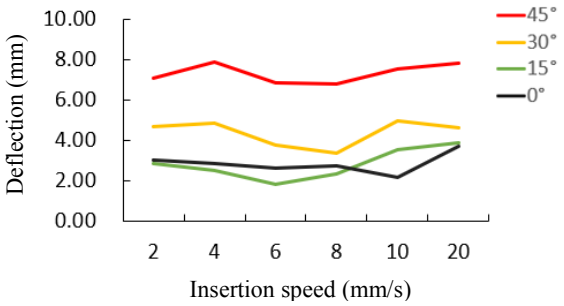

0° to 45° : Greenhouse-Geisser $p < 0.001$ **
0° and 15° : Bonferroni $p = 1.000$ n.s.(not significant)
15° and 30° : Bonferroni $p < 0.001$ **
30° and 45° : Bonferroni $p < 0.001$ **

Figure 7. Needle deflections due to the combination of insertion angles and insertion speeds in pig kidney. The legend in the upper right corner of the figure indicates the four insertion angles (0°, 15°, 30°, and 45°).

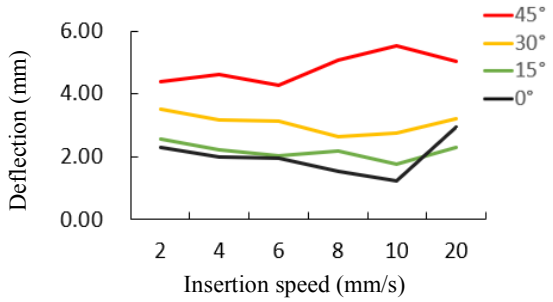

0° to 45° : Greenhouse-Geisser $p < 0.001$ **
0° and 15° : Bonferroni $p = 0.053$ n.s.(not significant)
15° and 30° : Bonferroni $p < 0.001$ **
30° and 45° : Bonferroni $p < 0.001$ **

Figure 8. Needle deflections due to the combination of insertion angles and insertion speeds in pig muscle. The legend in the upper right corner of the figure indicates the four insertion angles (0°, 15°, 30°, and 45°).

angles, such as 0° and 15°, and increased with larger insertion angles, such as 30° and 45°. In addition, the changing behavior of needle deflections with increasing insertion speeds was different for insertion angles. At the insertion angle of 0°, needle deflections were less than 2.5 mm only at 10 mm/s. At 15°, needle deflections were less than 2.5 mm only at 4, 6, and 8 mm/s. At other insertion speeds, needle deflections were greater than 2.5 mm. At 30° and 45°, needle deflections were greater than 2.5 mm.

E. Results on Pig Muscle

Fig. 8 illustrates the relationship between needle deflections and the combination of insertion speeds and insertion angles when pig muscle was punctured. The mean needle deflections were 1.99, 2.18, 3.07, and 4.82 mm for insertion angles at 0°, 15°, 30°, and 45°, respectively. The *p*-value for Gisser–Greenhouse correction from 0° to 45° was less than 0.001, noting a significant difference. In addition, the *p*-value of Bonferroni's multiple comparison test between 0° and 15° was 0.053, suggesting no significant difference. The *p*-value of Bonferroni's multiple comparison test between 15° and 30°, and 30° and 45° was less than 0.001, suggesting a significant difference. Thus, needle deflections were not significantly affected by small insertion angles, such as 0° and 15°, and increased with larger increasing insertion angles, such as 30° and 45°. Additionally, the changing behavior of needle deflections with increasing insertion speeds was different for insertion angles. At the insertion angle of 0°, needle deflections were less than 2.5 mm only at 2, 4, 6, 8, and 10 mm/s. At the insertion angle of 15°, needle deflections were less than 2.5 mm only at 4, 6, 8, 10, and 20 mm/s. At other insertion speeds, needle deflections were greater than 2.5 mm. At 30° and 45°, needle deflections were greater than 2.5 mm.

F. Discussion

As for pig fat and liver, needle deflections significantly increased with increasing insertion angles. These organs are soft. Therefore, they were thought to slide easily on the surface even at small insertion angles.

Regarding the pig kidney and muscle, no significant needle deflections were observed between 0° and 15°, but needle deflections increased with larger insertion angles above 15°. These organs are hard. Therefore, it was thought that the reaction force on the needle might stop it from slipping on the surface of these organs when the insertion angle was small.

IV. Derivation of the Optimal Insertion Speed

The relationship between the needle deflections and combined insertion speeds and insertion angles in the organs is then summarized. **Fig. 9** shows the mean needle deflections for various combination of insertion speeds and angles for each organ. In the case of a cancer tumor with a diameter of 10 mm, a needle deflection of 2.5 mm or less is sufficient. Meanwhile, a needle deflection of 5.0 mm is an acceptable critical value. Therefore, a needle deflection of 2.5 mm or less is indicated in green ("Recommended"), a needle deflection between 2.5 and 5.0 mm is indicated in yellow ("Acceptable"), and a needle deflection of 5.0 mm or more is indicated in red ("Unacceptable"). In addition, of the "Recommended" conditions for each insertion angle, the condition with the fastest insertion speed is marked as "Adoption" and with a red rectangle.

As for pig fat (**Fig. 9** (a)), since all conditions were labeled "Recommended" at the insertion angle of 0°, insertion at the

	Fat			
Angle	0°	15°	30°	45°
Speed	Deflection [mm]			
2mm/s	1.4	3.5	4.5	5.7
4mm/s	1.5	2.9	3.9	4.3
6mm/s	1.5	2.3	4.5	5.8
8mm/s	1.6	3.1	3.3	5.8
10mm/s	1.5	2.2	3.8	8.1
20mm/s	1.8	1.9	2.6	6.9

Recommended
Acceptable
Unacceptable
Adoption

(a) Pig fat

	Liver			
Angle	0°	15°	30°	45°
Speed	Deflection [mm]			
2mm/s	1.3	2.4	4.7	12.0
4mm/s	1.3	2.3	3.5	10.0
6mm/s	1.7	3.4	3.7	13.9
8mm/s	1.7	3.2	4.5	14.8
10mm/s	1.7	3.4	5.1	10.9
20mm/s	1.7	3.7	4.9	11.5

Recommended
Acceptable
Unacceptable
Adoption

(b) Pig liver

	Kidney			
Angle	0°	15°	30°	45°
Speed	Deflection [mm]			
2mm/s	3.1	2.8	4.7	7.1
4mm/s	2.9	2.5	4.9	7.9
6mm/s	2.6	1.8	3.8	6.8
8mm/s	2.8	2.3	3.4	6.8
10mm/s	2.2	3.6	4.9	7.5
20mm/s	3.7	3.9	4.6	7.8

Recommended
Acceptable
Unacceptable
Adoption

(c) Pig kidney

	Muscle			
Angle	0°	15°	30°	45°
Speed	Deflection [mm]			
2mm/s	2.3	2.6	3.5	4.4
4mm/s	2.0	2.2	3.2	4.6
6mm/s	2.0	2.0	3.1	4.3
8mm/s	1.5	2.2	2.6	5.1
10mm/s	1.2	1.8	2.7	5.5
20mm/s	2.9	2.3	3.2	5.0

Recommended
Acceptable
Unacceptable
Adoption

(d) Pig muscle

Figure 9. Mean needle deflections for combination of insertion speeds and angles for (a) fat, (b) liver, (c) kidney, and (d) muscle of pigs.

fastest insertion speed of 20 mm/s was both accurate and efficient. At 15°, insertion at 6, 10, and 20 mm/s were labeled "Recommended," so insertion at 20 mm/s, the fastest insertion speed, was the best way to achieve accuracy as well as efficiency.

As for the pig liver (**Fig. 9** (b)), since all conditions were labeled "Recommended" at the insertion angle of 0°, insertion at the fastest insertion speed of 20 mm/s was both accurate and efficient. At 15°, insertion at 2 and 4 mm/s were labeled "Recommended", so insertion at 4 mm/s, the fastest insertion speed, was the best way to achieve accuracy as well as efficiency.

As for the pig kidney (**Fig. 9** (c)), since a condition with an insertion speed of 10 mm/s was labeled "Recommended" at an insertion angle of 0°, insertion at the insertion speed of 10 mm/s was both accurate and efficient. At 15°, insertion at 4, 6, and 8 mm/s were labeled "Recommended", so insertion at 8 mm/s, the fastest insertion speed, was the best way to achieve accuracy as well as efficiency.

Regarding pig muscles (**Fig. 9** (d)), since conditions that insertion speeds were 2, 4, 6, 8, and 10 mm/s were labeled "Recommended" at an insertion angle of 0°, insertion at the fastest insertion speed of 10 mm/s was both accurate and efficient. At 15°, insertions at 4, 6, 8, 10 and 20 mm/s were labeled "Recommended", so insertion at 20 mm/s, which was the fastest insertion speed, was the best way to achieve accuracy as well as efficiency.

For all organs, insertion errors were observed to increase at larger angles of 30° and 45°. It is thought that larger angles increase the lateral reaction force at the needle tip, which increases deflection. On the other hand, when using angles such as 30° or 45° in practical use, it is necessary to take an angle that causes insertion errors in other organs in order to cancel insertion errors that occur in specific organs.

V. Conclusion

This study aimed to derive insertion speeds that could be both accurate and efficient for pig liver, kidney, fat, and muscle. Insertion tests were performed on each organ under conditions of 0° insertion angles and varying insertion speeds. There was no significant difference in deflections with increasing insertion speeds in pig fat or liver. A critical insertion speed minimizing needle deflections existed in pig kidney and muscle. These differences in the organ's characteristics were thought to be due to their differences in hardness. In addition, insertion tests were performed under conditions in which the insertion angles and the insertion speeds were varied. In the pig fat and liver, needle deflections significantly increased with increasing insertion angles. In the pig kidney and muscle, needle deflections significantly increased with increasing insertion angles above 15°. These results were used to derive the optimal insertion speed for puncturing the pig kidney, liver, fat, and muscle.

In the future, it is necessary to derive optimal insertion speed for the the other organs. Additionally, since it is desirable to use insertion planning in combination with organ segmentation techniques using CT images to select optimal insertion speed, the development and verification of the automatic insertion speed-setting system will be undertaken.

References

[1] K. Hasumi, Y. Aoki, R. Wantanabe, and D. Mann, "Clinical response of advanced cancer patients to cellular immunotherapy and intensity-modulated radiation therapy," Oncoimmunology, vol. 2, no. 10, p. e26381, 2013.

[2] I. Elgezua, Y. Kobayashi, and M. Fujie, "Survey on current state-of-the-art in needle insertion robots: Open challenges for application in real surgery," Procedia CIRP, vol. 5, pp. 94–99, 2013.

[3] H. Su et al., "Piezoelectrically actuated robotic system for MRI-guided prostate percutaneous therapy," IEEE ASME Trans. Mechatron., vol. 20, no. 4, pp. 1920–1932, Aug. 2015.

[4] E. Franco, D. Brujic, M. Rea, W. Gedroyc, and M. Ristic, "Needle-guiding robot for laser ablation of liver tumors under MRI guidance," IEEE/ASME Trans. Mechatron., vol. 21, no. 2, pp. 931–944, Apr. 2016.

[5] A. Majewicz et al., "Behavior of tip-steerable needles in ex vivo and in vivo tissue," IEEE Trans. Biomed Eng., vol. 59, no. 10, pp. 2705–2715, Oct. 2012.

[6] Y. Kobayashi et al., "Development of an integrated needle insertion system with image guidance and deformation simulation," Comput. Med. Imaging Graph., vol. 34, no. 1, pp. 9–18, 2010.

[7] R. Webster III et al., "Nonholonomic modelling of needle steering," Int. J. Robot. Res., vol. 25, nos. 5/6, pp. 509–525, 2006.

[8] M. Abayazid et al., "Ultrasound-guided three-dimensional needle steering in biological tissue with curved surfaces," Med. Eng. Phys., vol. 37, no. 1, pp. 145–150, 2015.

[9] G. Vrooijink, M. Abayazid, S. Patil, R. Alterovitz, and S. Misra, "Needle path planning and steering in a three-dimensional non-static environment using two-dimensional ultrasound images," Int. J. Rob. Res., vol. 33, no. 10, 1361–1374, 2014.

[10] H. Lee and J. Kim, "Estimation of flexible needle deflection in layered soft tissues with different elastic moduli," Med. Biol. Eng. Comput., vol. 52, no. 9, pp. 729–740, 2014.

[11] M. Khadem et al., "A mechanics-based model for simulation and control of flexible needle insertion in soft tissue," In Proc. IEEE Int. Conf. Robot. Autom., 2015, pp. 2264–2269.

[12] S. Misra, K. Reed, B. Schafer, K. Ramesh, and A. Okamura, "Mechanics of flexible needles robotically steered through soft tissue," Int. J. Rob. Res., vol. 29, no. 13, pp. 1640–1660, 2010.

[13] R. Tsumura, Y. Takishita, and H. Iwata, "Needle insertion control method for minimizing both deflections and tissue damage," J. Med. Robot. Res., vol. 3, no. 4, pp. 1842005-1-9, 2018.

[14] R. Tsumura, K. Shitashima, and H. Iwata, "Insertion method for minimizing fine needle deflection in bowel insertion based on experimental analysis," IEEE Int. Conf. Intell. Robot. Syst., 2017, pp. 187–192.

[15] R. Tsumura, I. Iordachita, and H. Iwata, "Fine needle insertion method for minimising deflection in lower abdomen: In vivo evaluation," Int. J. Med. Robot., vol. 16, no. 6, 1–12, 2020.

[16] R. Tsumura, J. Kim, H. Iwata, and I. Iordachita, "Preoperative needle insertion path planning for minimizing deflection in multilayered tissues," IEEE Robot. Autom. Lett., vol. 3, no. 3, pp. 2129–2136, 2018.

[17] N. Abolhassani, R. Patel, and F. Ayazi, "Effects of different insertion methods on reducing needle deflection," 2007 29th Annual International Conference of the IEEE Engineering in Medicine and Biology Society, pp. 491–494, Aug. 2007, ISSN 1558-4615.

[18] C. McGill, J. Schwartz, J. Moore, P. McLaughlin, and A. Shih, "Effects of insertion speed and trocar stiffness on the accuracy of needle position for brachytherapy," Med. Phys., vol. 39, no. 4, pp. 1811–1817, 2012.

[19] A. Jahya, F. Van der Heijden, and S. Misra, "Observations of three-dimensional needle deflection during insertion into soft tissue," In Proceedings of the 4th IEEE/ras-EMBS international conference on biomedical robotics and Biomechatronics (BioRob), Rome, Italy, 2012, pp. 1205–1210.

[20] T. Podder, D. Clark, D. Fuller, J. Sherman, and Y. Yu, "Effects of Velocity Modulation during surgical needle insertion," IEEE Eng. Med. Biol. 27th Annual Conference, pp. 5766–5770, 2005.

[21] X. Dai, Y. Zhang, J. Jiang, and S. Zhang, "A needle deflection model with operating condition optimization for corrective force-based needle guidance during transrectal prostate brachytherapy," Int. J. Med. Robot., vol. 18, no. 3, p. e2388, 2022.